# Mesoscopic Theory of Resistive Switching

E. Miranda, *Senior Member, IEEE*, and J. Suñé, *Fellow, IEEE*

***Abstract*— The quantum nature of filamentary-type resistive switching (RS) occurring in thin oxide films has been investigated for more than two decades and though the key concepts for a mesoscopic theory of RS are well known, establishing a simple phenomenological model consistent with the experimental observations has proven to be an elusive task. The physics of RS is complex because it involves the coupled action of electrons and ions or vacancies, a connection which gives rise to the hysteretic behavior of the conduction characteristic of the device. In this letter, a model based on the Landauer approach for the electron transport through a narrow constriction is revisited and combined with the master equation for the generation and dissolution of a nanosized gap. The proposed model not only sheds light on one of the most widely invoked equations for conduction in RS devices (Stanford-PKU RRAM model) but also provides the physical meaning of its parameters. The role played by the power dissipation at the two ends of the constriction during the occurrence of the switching process is also discussed.**

***Index Terms*— Memristor, resistive switching, mesoscopic.**

## I. Introduction

FILAMENTARY-TYPE conduction in resistive switching (RS) devices has been extensively investigated in the last years [1]. The appearance of this filament is linked to the local accumulation (electroforming) of metal ions or oxygen vacancies forming a kind of conducting bridge across a thin dielectric film sandwiched in between two metal electrodes. Since the filament can be alternately created and destroyed by the application of a proper external electrical stimulus, the resulting resistance change can be used to store information in a nonvolatile fashion. The control of the device conductance (synaptic weight) is also of utmost importance in the field of neuromorphic computing [2], [3]. It has been reported several times that the electron transport in RS devices exhibits quantum effects [4], [5], [6], [7], [8], [9], the most striking manifestation being the observation of conductance jumps of the order of the quantum unit $G_0 = 2e^2/h$, where $e$ is the electron charge and $h$ the Planck constant. These jumps have been attributed to structural modifications of the filament atomic configuration [10]. The physical system is often referred to as a quantum point contact (QPC) [11] and its connection with dielectric breakdown has been matter of intense research in the past [12], [13]. In this letter, we adopt the modeling framework of memristive devices [14], *i.e.* a system of two coupled equations, one for the current-voltage characteristic (Landauer approach) and one for the memory state (master equation). For simplicity, we focus here on the canonical case of a single filament with internal progressive dynamics but the extension to abrupt transitions or multiple non-interacting filaments is straightforward.

Manuscript received 17 June 2024; revised 27 July 2024 and 30 July 2024; accepted 7 August 2024. Date of publication 13 August 2024; date of current version 27 September 2024. This work was supported by the Ministerio de Ciencia, Innovación y Universidades (MCIN)/Agencia Española de Investigación (AEI)/10.13039/501100011033 under Project PID2022-139586NBC41. The review of this letter was arranged by Editor V. Moroz. *(Corresponding author: E. Miranda.)*

The authors are with the Departament d'Enginyeria Electrònica, Universitat Autònoma de Barcelona, 08193 Bellaterra, Spain (e-mail: enrique.miranda@uab.cat).

Color versions of one or more figures in this letter are available at https://doi.org/10.1109/LED.2024.3442818.

Digital Object Identifier 10.1109/LED.2024.3442818

## II. Model for the Current-Voltage Characteristic

According to the finite-bias Landauer approach for mesoscopic conductors [15], the $I$-$V$ characteristic of a symmetric QPC structure can be calculated using the expression:

$$I(V) = \frac{2e}{h}\int_{-\infty}^{\infty} D(\varepsilon)\left\{f\left[\varepsilon-\mu_L\right]-f\left[\varepsilon-\mu_R\right]\right\}d\varepsilon \quad (1)$$

where $\varepsilon$ is the energy, $D$ the transmission probability, $f$ the Fermi-Dirac function, and $\mu_L = eV/2$, $\mu_R = -eV/2$ the electrochemical potentials at the left and right sides of the constriction, respectively. Assuming a 1D inverted parabolic barrier of height $\varphi$ at $z = 0$ for the first energy subband in the constriction's bottleneck (see Fig. 1a):

$$\Psi(z) \approx \varphi - \frac{1}{2}m\omega^2 z^2 \quad (2)$$

the exact expression for $D$ reads [16]:

$$D(\varepsilon) = \frac{1}{1+e^{-\alpha(\varepsilon-\varphi)}} \quad (3)$$

where $\alpha$ is a constant related to the curvature $k=\omega^2 m$ of the potential barrier profile. Notice that, in this representation, $\Psi$ is not a material-related barrier but a barrier that arises from the quantum confinement of the electron wavefunction. In terms of the geometry of the constriction, namely its gap size $g$[m] (roughly the separation between the two roots of Eq.(2)) and radius $R$[m] (considering an infinite cylindrical quantum well), $\alpha$[1/eV] and $\varphi$[eV] read [17]:

$$\alpha = \frac{2\pi}{\hbar\omega} = \frac{g}{2\hbar}\sqrt{\frac{2m}{\varphi}} = \frac{\pi m}{\hbar^2 z_o}gR \quad (4)$$

$$\varphi = \frac{\hbar^2 z_o^2}{2m}\frac{1}{R^2} \quad (5)$$

where $m$[eV/c$^2$] is the effective electron mass in the constriction and $z_0 = 2.405$ the first root of the Bessel function $J_0$ [18]. The physical units are indicated within brackets. In the zero-temperature limit, (1) can be fully integrated [19], but for the sake of simplicity let us consider here the case $eV/2 < \varphi$, *i.e.* the tunneling regime. In this case, (1) yields:

$$I(V) = \frac{4e}{\alpha h}e^{-\alpha\varphi}\sinh\left(\frac{e\alpha}{2}V\right) \quad (6)$$

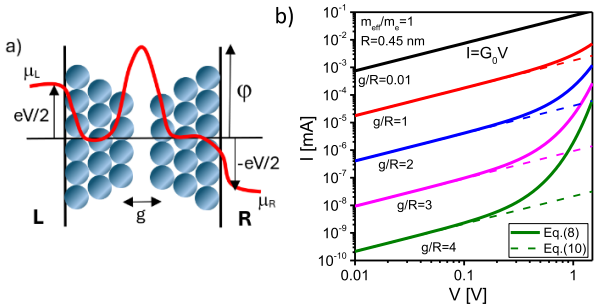


Fig. 1. a) Schematics of the energy barrier model for the quantum confinement effect in the filament. *L* and *R* refer to the left and right electrodes, respectively. *g* is the gap width and $\varphi$ the top of the potential barrier. b) *I-V* characteristics in log-log scale for different *g*/*R* aspect ratios (see Eq.(7)). $m/m_e$ is the effective electron mass ratio.

Notice that the product of the fitting parameters $\alpha\varphi$ in (6) is directly related to the aspect ratio of the constriction $g/R$ and is independent of $m$:

$$\frac{g}{R} = \frac{2}{\pi z_0}\alpha\varphi \tag{7}$$

Remarkably, (6) can be alternatively expressed as:

$$I\,(V) = I_0 e^{-\frac{g}{g_0}} \sinh\left(\frac{V}{V_0}\right) \tag{8}$$

with:

$$I_0\,[\mathrm{A}] = G_0 V_0,\; g_0\,[\mathrm{m}] = \frac{2}{\pi z_0} R,\; V_0[\mathrm{V}] = \frac{2\hbar^2 z_0}{e\pi m}\frac{1}{Rg} \tag{9}$$

(8) is the well-known expression for the *I-V* curve implemented in the Stanford-PKU model for RS devices [20]. Now, the dependence of the model electrical parameters $I_0$, $g_0$ and $V_0$ on the physical parameters $g$, $R$ and $m$ is clearly revealed. Both (6) and (8) are convenient expressions since they comply with the expected limit for the conductance of a collapsing barrier $G(\alpha, g \to 0) = G_0$ (see Fig. 1b). In this limit, the *I-V* curve is linear rather than exponential as predicted by the Landauer formula (see Fig. 1b). Similar results can be obtained assuming a wide constriction (large $R$), *i.e.* the absence of a confinement barrier, since also in this case $D \to 1$. Interestingly, considering $V \ll V_0$ (very low bias) and $sinh(x) \approx x$, (8) reads:

$$G = \frac{dI}{dV} \approx G_0 e^{-\frac{g}{g_0}} \tag{10}$$

which is the expression for the conductance of a mesoscopic bridge obtained from first principle calculations [21]. In particular $g_0 = 0.12$ nm has been found for $HfO_2$ [21], so that from (9), $R = 0.45$ nm is obtained. More recent results seem to indicate that $g_0$ depends on the particular properties of the oxide layer [22]. Since we are dealing with a non-purely electronic phenomenon, a second physical mechanism needs to be introduced in order to account for the hysteretic behavior in the conduction characteristic of RS devices.

## III. Model for the Memory State of the Device

For the memory state of the device, let's consider the master equation corresponding to a birth-death process [23]. We assume here that the particles able to form the atomic bridge at the constriction's bottleneck can be alternatively in two states: conducting (A) or non-conducting (B), a kind of redox process in VCMs or a local displacement of metal ions in ECMs. We assume also that the total number of particles $N$ within the region of interest is constant, *i.e.* $n_A + n_B = N$, where $n_A$ and $n_B$ are the number of particles in states A and B, respectively. The switching of one particle from one state to the other is mainly driven by the average electric field across the dielectric film which is initially assumed constant. If $\omega_{ij}$ is the transition rate from state $i$ to state $j$ then, neglecting second order terms in $\Delta t$, the following textbook gain-loss equations describes the occupation probabilities of both states [24]:

$$\frac{dP\,(n_i, t)}{dt} = \sum_{i \neq j = A,B} \left[-\omega_{ij} P\,(n_i, t) + \omega_{ji} P\,(n_j, t)\right] \tag{11}$$

where $P\,(n_A, t) + P\,(n_B, t) = 1, \forall t$. The master equation (11) can be solved with the aid of the binomial distribution or more in general with the generating function $G$ defined as:

$$G(s, t) = \sum_{n=-\infty}^{\infty} s^n P(n, t) \tag{12}$$

The series expansion (12) allows the easy calculation of the first moment of the random variable $n_A$ as:

$$\langle n_A(t)\rangle = \sum_{n_A} n_A P\,(n_A, t) = \left.\frac{\partial G(s, t)}{\partial s}\right|_{s=1} \tag{13}$$

where

$$G\,(s, t) = \left\{\frac{\omega_S\left[s + e^{-\omega t}\,(1 - s)\right] + \omega_R}{\omega}\right\}^N \tag{14}$$

In our case, $\omega = \omega_S + \omega_R$, $\omega_S$ and $\omega_R$ being the set (B→A) and reset (A→B) transition rates, respectively, expressed as [25]:

$$\omega_S\,(V) = \omega_{0S} sinh\left(\frac{V}{V_{0S}}\right) H(V) \tag{15}$$

$$\omega_R\,(V) = \omega_{0R} sinh\left(-\frac{V}{V_{0R}}\right) H(-V) \tag{16}$$

$\omega_{0S}$, $\omega_{0R}$, $V_{0S}$ and $V_{0R}$ are model constants and $H$ the Heaviside function. (15) and (16) correspond to transition rates of vacancies or drift coefficients of metal ions in the oxide layer. The hyperbolic sine eliminates the problem of a non-zero transition rate at $V = 0$. From (13)-(16), the transparency of the constriction $0 \leq \rho \leq 1$ is defined as:

$$\rho(t) = \frac{\langle n_A(t)\rangle}{N} = \frac{\omega_S}{\omega}\left[1 - e^{-\omega t}\right] + \rho_0 e^{-\omega t}, \tag{17}$$

*i.e.* the normalized number of conducting particles. $\rho_0$is the initial condition for $\rho(t)$. Figure 2a illustrates $\rho(t)$ for typical potentiation ($V > 0$) and depression ($V < 0$) cases as a function of time and applied voltage. A similar expression can be written for the non-conducting species but the use of (17) is more convenient for the sake of clarity.

## IV. Mean-Field Approximation and Model Equations

Assuming that the gap size $g$ shrinks as the constriction's transparency $\rho$ increases, we make the following ansatz for the normalized gap length:

$$\tilde{g}(t) = \frac{g\,(t) - g_m}{g_M - g_m} = 1 - \rho(t) \tag{18}$$

where $g_m$ and $g_M$ are the minimum and maximum gap lengths, respectively. From the mean-field theory of master equations (fluctuations are neglected), (11) and (17) allow establishing the deterministic differential equation:

$$\frac{d\tilde{g}}{dt} = -\omega_S \tilde{g} + \omega_R\,(1 - \tilde{g}) \tag{19}$$

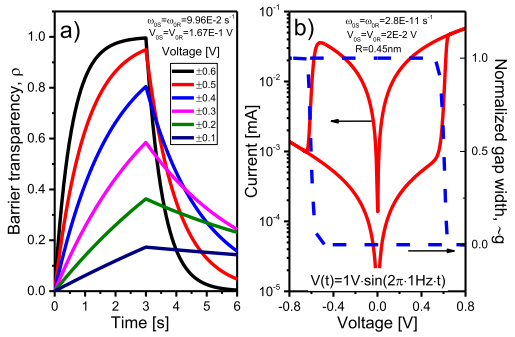


Fig. 2. a) Simulation of the potentiation (V>0) and depression (V<0) effects in the constriction transparency factor using expression (17). b) Typical *I-V* loop and evolution of the normalized gap width corresponding to the RS mechanism obtained from expressions (8) and (19).

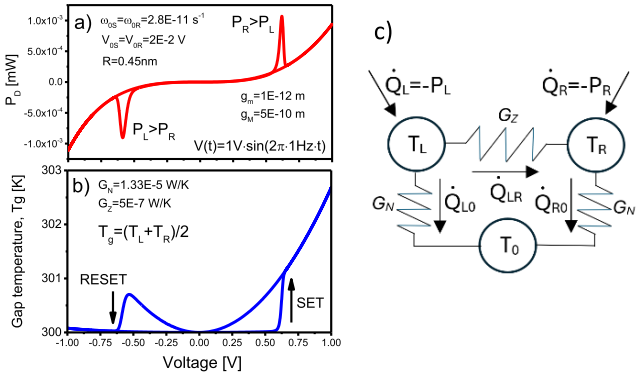


Fig. 3. a) Difference in the dissipated power ($P_D$◁ as a function of the applied voltage during the opening and closing of a quantum channel. b) Temperature at the gap. c) Equivalent thermal model for the QPC structure.

which expresses the evolution of the gap width as a function of time. Notice that the similarity between (11) and (19) is not a coincidence, since (19) represents the macroscopic (average) version of (11). However, in some extent, (19) increases the scope of (17) because the transition rates do not longer need to be considered constants, *i.e.* arbitrary voltage signals are now allowed. This is illustrated in Fig. 2b for the case of a sinusoidal signal. As can be seeen, the collapse of the gap is reflected in a notable current increase. The subsequent formation of the gap at a negative bias generates the reset transition. In summary, the proposed mesoscopic model for RS devices is finally expressed by equations (8) and (19).

## V. On the Asymmetry of Power Dissipation

In this Section, we discuss how power dissipates at the two ends of the constriction during the switching cycle and the effect on the gap temperature, $T_g$. Assuming a quasi-static approach, power dissipation at the left ($L$) and right ($R$) sides of the constriction can be calculated according to (see Fig. 1a):

$$P_L = \frac{2}{h}\int_{-\infty}^{\infty}(\mu_L-\varepsilon)\,D(\varepsilon)\,\{f[\varepsilon-\mu_L]-f[\varepsilon-\mu_R]\}\,d\varepsilon$$
$$= \frac{2e}{h\alpha^2}e^{-\alpha\varphi}\left[e^{\alpha eV/2}-(1+\alpha eV)e^{-\alpha eV/2}\right] \quad (20)$$

$$P_R = \frac{2}{h}\int_{-\infty}^{\infty}(\varepsilon-\mu_R)\,D(\varepsilon)\,\{f[\varepsilon-\mu_L]-f[\varepsilon-\mu_R]\}\,d\varepsilon$$
$$= \frac{2e}{h\alpha^2}e^{-\alpha\varphi}\left[e^{-\alpha eV/2}-(1-\alpha eV)e^{\alpha eV/2}\right] \quad (21)$$

As expected, $P_S = P_R + P_L = IV$, which corresponds to the power dissipated in the device. We still assume that the spread of the Fermi-Dirac functions at the electrodes is negligible and that we are operating in the tunneling regime [26]. However, if we focus the attention instead on the difference $P_D = P_R$-$P_L$, we obtain from (20) and (21):

$$P_D = \frac{2e}{h\alpha^2}e^{-\alpha\varphi}\left[(\alpha eV-2)\,e^{\alpha eV/2}+(\alpha eV+2)\,e^{-\alpha eV/2}\right] \quad (22)$$

As illustrated in Fig. 3a, the formation and destruction of a $G_0$ conductance channel are associated with a strong asymmetry of the energy release in the device. This occurs because of the exponential dependence of $D$ on $\varepsilon$ and has been the subject of recent investigations in QPCs [27]. Dissipation is always higher at the drain electrode (where electrons thermalize). This indicates that although the electron transport in the constriction is elastic, a heat current $dQ_{LR}/dt$=$G_z(T_L$-$T_R)$ flows across the gap generating a thermal gradient [28]. $T_R$ and $T_L$ are the temperatures at the two sides of the constriction and $G_z$ = 5E-7K/W [29] the thermal conductance in the $z$ direction. The equivalent thermal circuit (see Fig. 3c) can be expressed as:

$$P_L = G_N\,(T_L-T_0)+G_z\,(T_L-T_R)$$
$$P_R = -G_z\,(T_L-T_R)+G_N\,(T_R-T_0) \quad (23)$$

where $G_N$ =1.33E-5W/K [29] is the thermal conductance in the normal direction to the electron flow and $T_0$ =300K the substrate temperature. From (23), the average temperature $T_g \approx (T_R+T_L)/2 = P_S/(2G_N)+T_0$ is computed and showed in Fig. 3b. This expression demonstrates how the power dissipated in the device relates to $T_g$, a well-known result. Thermal inertia has not been considered here. It is speculated that for larger currents than those considered in this canonical case, the generated heat wave facilitates the ion or vacancy migration in bipolar RS devices as widely suggested in the literature [30]. In this connection, the Soret effect can play a role in the movement of the atomic species [31].

## VI. Conclusion

Observation of quantum effects in the hysteretic conduction characteristics of RS devices is no longer considered as a mere artifact. The phenomenon has been reported many times and it is not associated with a single specific material or device. It is the consequence of the funneling of the electron wavefunction when passing through a narrow constriction of atomic dimensions. In this letter, we revisited the QPC model for the electron transport in broken down dielectrics and we linked it to the Stanford-PKU model for RS devices. In this way, we were able to determine the physical meaning of its parameters. In addition, we connected this model with the master equation describing the formation and destruction of the gap along the filamentary structure. Finally, we demonstrated that the opening and closing of a quantum channel generate a large asymmetry in the spatial distribution of the dissipated power which can ultimately contribute to the movement of the atomic species.

## References

[1] R. Waser, R. Dittmann, G. Staikov, and K. Szot, "Redox-based resistive switching memories–nanoionic mechanisms, prospects, and challenges," *Adv. Mater.*, vol. 21, nos. 25–26, pp. 2632–2663, Jul. 2009, doi: 10.1002/adma.200900375.

[2] J. Zhu, T. Zhang, Y. Yang, and R. Huang, "A comprehensive review on emerging artificial neuromorphic devices," *Appl. Phys. Rev.*, vol. 7, no. 1, Mar. 2020, Art. no. 011312, doi: 10.1063/1.5118217.

[3] D. Ielmini, Z. Wang, and Y. Liu, "Brain-inspired computing via memory device physics," *APL Mater.*, vol. 9, no. 5, May 2021, Art. no. 050702, doi: 10.1063/5.0047641.

[4] Y. Li, S. Long, Y. Liu, C. Hu, J. Teng, Q. Liu, H. Lv, J. Suñé, and M. Liu, "Conductance quantization in resistive random access memory," *Nanosc. Res. Lett.*, vol. 10, no. 1, p. 420, Dec. 2015, doi: 10.1186/s11671-015-1118-6.

[5] W. Xue, S. Gao, J. Shang, X. Yi, G. Liu, and R. Li, "Recent advances of quantum conductance in memristors," *Adv. Electron. Mater.*, vol. 5, no. 9, Sep. 2019, Art. no. 1800854, doi: 10.1002/aelm.201800854.

[6] J. M. M. Andrade, C. M. M. Rosário, S. Menzel, R. Waser, and N. A. Sobolev, "Application of the quantum-point-contact formalism to model the filamentary conduction in $Ta_2O_5$-based resistive switching devices," *Phys. Rev. Appl.*, vol. 17, no. 3, Mar. 2022, Art. no. 034062, doi: 10.1103/physrevapplied.17.034062.

[7] G. Milano, M. Aono, L. Boarino, U. Celano, T. Hasegawa, M. Kozicki, S. Majumdar, M. Menghini E. Miranda, C. Ricciardi, S. Tappertzhofen, K. Terabe, and I. Valov, "Quantum conductance in memristive devices: Fundamentals, developments, and applications," *Adv. Mater.*, vol. 34, Apr. 2022, Art. no. 2201248, doi: 10.1002/adma.202270235.

[8] J. Suñé, F. Aguirre, M. Bargalló González, F. Campabadal, and E. Miranda, "Exploring conductance quantization effects in electroformed filaments for their potential application to a resistance standard," *Adv. Quantum Technol.*, vol. 6, no. 7, Jul. 2023, Art. no. 2300048, doi: 10.1002/qute.202300048.

[9] F. L. Aguirre, E. Piros, N. Kaiser, T. Vogel, S. Petzold, J. Gehrunger, C. Hochberger, T. Oster, K. Hofmann, J. Suñé, E. Miranda, and L. Alff, "Revealing the quantum nature of the voltage-induced conductance changes in oxygen engineered yttrium oxide-based RRAM devices," *Sci. Rep.*, vol. 14, no. 1, p. 1122, Jan. 2024, doi: 10.1038/s41598-023-49924-2.

[10] K. Krishnan, M. Muruganathan, T. Tsuruoka, H. Mizuta, and M. Aono, "Quantized conductance operation near a single-atom point contact in a polymer-based atomic switch," *Jpn. J. Appl. Phys.*, vol. 56, no. 6S1, Jun. 2017, Art. no. 06GF02, doi: 10.7567/jjap.56.06gf02.

[11] H. van Houten and C. Beenakker, "Quantum point contacts," *Phys. Today*, vol. 49, no. 7, pp. 22–27, Jul. 1996, doi: 10.1063/1.881503.

[12] J. Sune, E. Miranda, M. Nafria, and X. Aymerich, "Point contact conduction at the oxide breakdown of MOS devices," in *IEDM Tech. Dig.*, Piscataway, NJ, USA, 1998, pp. 191–194, doi: 10.1109/IEDM.1998.746318.

[13] E. Miranda and J. Suñé, "Electron transport through broken down ultra-thin $SiO_2$ layers in MOS devices," *Microelectron. Rel.*, vol. 44, no. 1, pp. 1–23, Jan. 2004, doi: 10.1016/j.microrel.2003.08.005.

[14] L. Chua, "Resistance switching memories are memristors," *Appl. Phys. A, Solids Surf.*, vol. 102, no. 4, pp. 765–783, Jan. 2011, doi: 10.1007/s00339-011-6264-9.

[15] S. Datta *Electronic Transport in Mesoscopic Systems*. Cambridge, U.K.: Cambridge Univ. Press, 1995, doi: 10.1017/CBO9780511805776.

[16] D. M. Heim, W. P. Schleich, P. M. Alsing, J. P. Dahl, and S. Varro, "Tunneling of an energy eigenstate through a parabolic barrier viewed from Wigner phase space," *Phys. Lett. A*, vol. 377, nos. 31–33, pp. 1822–1825, Oct. 2013, doi: 10.1016/j.physleta.2013.05.017.

[17] E. Miranda, D. Jimenez, and J. Sune, "The quantum point-contact memristor," *IEEE Electron Device Lett.*, vol. 33, no. 10, pp. 1474–1476, Oct. 2012, doi: 10.1109/LED.2012.2210185.

[18] G. Gulyamov, A. G. Gulyamov, A. B. Davlatov, and B. B. Shahobiddinov, "Electron energy in rectangular and cylindrical quantum wires," *J. Nano-Electron. Phys.*, vol. 12, no. 4, 2020, Art. no. 04023, doi: 10.21272/jnep.12(4).04023.

[19] E. A. Miranda, C. Walczyk, C. Wenger, and T. Schroeder, "Model for the resistive switching effect in $HfO_2$ MIM structures based on the transmission properties of narrow constrictions," *IEEE Electron Device Lett.*, vol. 31, no. 6, pp. 609–611, Jun. 2010, doi: 10.1109/LED.2010.2046310.

[20] Z. Jiang, Y. Wu, S. Yu, L. Yang, K. Song, Z. Karim, and H.-S. P. Wong, "A compact model for metal–oxide resistive random access memory with experiment verification," *IEEE Trans. Electron Devices*, vol. 63, no. 5, pp. 1884–1892, May 2016, doi: 10.1109/TED.2016.2545412.

[21] X. Lian, X. Cartoixà, E. Miranda, L. Perniola, R. Rurali, S. Long, M. Liu, and J. Suñé, "Multi-scale quantum point contact model for filamentary conduction in resistive random access memories devices," *J. Appl. Phys.*, vol. 115, no. 24, Jun. 2014, Art. no. 244507, doi: 10.1063/1.4885419.

[22] J. Reuben, D. Fey, and C. Wenger, "A modeling methodology for resistive RAM based on stanford-PKU model with extended multilevel capability," *IEEE Trans. Nanotechnol.*, vol. 18, pp. 647–656, 2019, doi: 10.1109/TNANO.2019.2922838.

[23] C. Gardiner, *Handbook of Stochastic Methods: For Physics. Chemistry, and the Natural Sciences* (Springer Series in Synergetics). Berlin, Germany: Springer, 1986.

[24] G. Haag, *Modelling With the Master Equation*. Cham, Switzerland: Springer, 2017, doi: 10.1007/978-3-319-60300-1.

[25] A. Rodriguez-Fernandez, J. Muñoz-Gorriz, J. Suñé, and E. Miranda, "A new method for estimating the conductive filament temperature in OxRAM devices based on escape rate theory," *Microelectron. Rel.*, vols. 88–90, pp. 142–146, Sep. 2018, doi: 10.1016/j.microrel.2018.06.120.

[26] A. Avellán, E. Miranda, D. Schroeder, and W. Krautschneider, "Model for the voltage and temperature dependence of the soft breakdown current in ultrathin gate oxides," *J. Appl. Phys.*, vol. 97, no. 1, Jan. 2005, Art. no. 014104, doi: 10.1063/1.1827343.

[27] C. Blaas-Anselmi, F. Helluin, R. Jalabert, G. Weick, and D. Weinmann, "Asymmetric power dissipation in electronic transport through a quantum point contact," *SciPost Phys.*, vol. 12, no. 3, p. 105, Mar. 2022, doi: 10.21468/scipostphys.12.3.105.

[28] J. P. Pekola and B. Karimi, "Colloquium: Quantum heat transport in condensed matter systems," *Rev. Modern Phys.*, vol. 93, no. 4, Oct. 2021, Art. no. 041001, doi: 10.1103/revmodphys.93.041001.

[29] J. Suñé, M. Bargalló-González, M. Saludes, F. Campabadal, and E. Miranda, "Event-driven stochastic compact model for resistive switching devices," *IEEE Trans. Electron Devices*, vol. 71, no. 8, pp. 4649–4654, Aug. 2024, doi: 10.1109/TED.2024.3414370.

[30] C. Aguilera-Pedregosa, D. Maldonado, M. B. González, E. Moreno, F. Jiménez-Molinos, F. Campabadal, and J. B. Roldán, "Thermal characterization of conductive filaments in unipolar resistive memories," *Micromachines*, vol. 14, no. 3, p. 630, Mar. 2023, doi: 10.3390/mi14030630.

[31] D. B. Strukov, F. Alibart, and R. Stanley Williams, "Thermophoresis/diffusion as a plausible mechanism for unipolar resistive switching in metal–oxide–metal memristors," *Appl. Phys. A, Solids Surf.*, vol. 107, no. 3, pp. 509–518, Jun. 2012, doi: 10.1007/s00339-012-6902-x.